Adsorption 6, 125–136, 2000

Analysis of Diffusion in Hollow Geometries

YAPING LÜ AND MARTIN BÜLOW
The BOC Group Gases Technology, 100 Mountain Avenue, Murray Hill, NJ 07974, USA

Received September 16, 1999; Revised February 3, 2000; Accepted February 8, 2000

Abstract. The diffusion in hollow particles of solid adsorbent materials was analyzed based on analytical solutions to the basic diffusion equation. Three geometric shapes (plane sheet, cylinder, and sphere) of sorbent material were considered for two kinds of boundary conditions. The equations for determining the equivalent sizes compared to their corresponding solid particles were obtained directly from the theoretical expressions of sorption uptake curves. Among the three hollow particles of impermeable inner surface, the sphere gives the highest gain in effective diffusion rate compared to the corresponding solid particle. For permeable inner surface, at lower hollow volume fractions, the plane sheet shows the highest gain, while at higher hollow volume fractions, the sphere shows the highest gain in effective diffusion rate.

Keywords: diffusion, mathematical model, analytical solution, hollow material, composite material, mass transfer

Background

Composite and hollow materials have a potential for applications as catalysts and sorbents in catalytic and adsorption processes. Examples of these types of materials include shell catalysts (Papa et al., 1991), natural materials for extraction and leaching (Sovova, 1994), pellicular adsorbents with inner core such as HPLC packing or microcapsule. Tosheva et al. (1999) prepared bilayered hollow zeolite tubes consisting of ZSM-5 and silicalite-1 with controlled length and wall thickness. Tatlier and Eerdem-Senatalar (1999) discussed the effect of the thickness of Zeolite 4A coating grown on metal surfaces for heat pump applications. Synthesis of clusters of acicular MFI zeolites from porous silica layers strongly attached to stainless steel surfaces was also reported by van der Eerden et al. (1999) for the use in catalysis.

Patent literature refers mainly to large-scale manufacture of particles with hollow shapes as well as with essentially non-porous cores. Examples are given as follows. US Patent 5,316,993 (Sextl and Kleinschmit, 1994) describes a process of producing hollow cylinders and tubular particles containing dealuminated Y-type zeolite materials. A similar procedure was described in the European Patent EP 0,309,048 A1 (Shell Internationale, 1989) for manufacturing moulded silicalite particles for purposes of adsorption or catalysis. A procedure consisting of press-shaping followed by sintering (Seki et al., 1989; Hublitz and Birkenstock, 1990) was also reported to prepare hollow sorbent macro particles and hollow ceramics particles that are useful for manufacture of filters, catalyst carriers, electrodes and electrolyte-retaining materials for fuel cells.

Specific sintering processes for open, moulded ceramic macro particles with various shapes have been claimed by the Schott Glaswerke of Germany (Siebers et al., 1989) and by Kabushiki Kaisha Osaka of Japan (Takahashi et al., 1990). Principles to form sintered polycrystalline bodies with extremely high density as referred to the theoretically possible value ($>95\%$) which could be used as solid impermeable cores are described in numerous patent applications, e.g., in Nippon Steel Corp. (1989) and Hunold et al. (1989). A further step would be "anchoring" (funtionalization of solid surfaces) of chemically reactive functional groups at the surface of those impermeable cores to enhance seeding of microporous solids. A variety of

mechanical conditions and chemical procedures of "anchoring" is well known from the art of preparation of columns for HPLC and other types of chromatography (Unger, 1989). A process of manufacture of hollow cylinder extrudates where the hollow cylinder could be made of nearly non-porous alumina, is described in EP 0,141,997,A1 (Pereira and Hegedus, 1985). Epitaxial growth of "metastable" structures on impermeable hard cores of a great variety of chemical species after appropriate "templating" the surfaces of the latter ones maybe envisaged as a first substantial step to microporous layers into which those "metastable" structures could be transferred.

Since diffusion of sorbing species does not take place in the inner layer of composite sorbent materials with a non-porous core (such as metal), the analysis of such a composite material is essentially the same as that for a hollow material. Carslaw and Jaeger (1959) gave the solutions to the diffusion equation for a hollow cylinder with general boundary conditions and the general solution to the problem of hollow sphere with both inner and outer surface maintained at constant concentration. A number of special cases were considered by Barrer (1944), who also suggested some practical systems to which the solutions could be applied. Goto and Hirose (1994) developed an approximate model for diffusion problems by the parabolic profile approximation for particles with inner cores, where only the outer shell region of a particle is available for diffusion.

Analysis and comparison of diffusion in hollow material geometries can provide the essential information for understanding the mass transfer behavior in such systems. In this study, the mass transfer coefficients were evaluated based on the analytical solutions to the diffusion equation for hollow materials of three geometrical shapes and two different inner boundary conditions, and mass transfer rates were compared between materials with hollow and solid geometries.

Analytical Solutions to the Diffusion Equations for Hollow Spheres

The analysis of the diffusion in hollow materials presented here is limited to three basic, one-dimensional cases with constant diffusion coefficient and isothermal condition. In doing so, the diffusion equations can be solved analytically, and the mathematical forms of the solutions are relatively simple. The three geometries considered are plane sheet (slab), cylinder, and sphere. The diffusion equations for these three geometries were solved analytically under the conditions of uniform initial concentration profile and constant external surface concentration. As far as the inner surface is concerned, two types of boundary conditions were examined. For the first type (Type I), the inner surface is impermeable to the diffusing species (or zero concentration gradient at the inner surface), while for the second type (Type II) constant concentration is assumed at the inner surface. The case of hollow sphere, for which the solution of impermeable inner surface is not available in the literature, will be given first and treated in more detail.

The equation for the diffusion in the radial direction with constant diffusion coefficient assumes the form

$$\frac{\partial C}{\partial t} = D\left(\frac{\partial^2 C}{\partial r^2} + \frac{2}{r}\frac{\partial C}{\partial r}\right). \tag{1}$$

Let us consider the diffusion in a hollow sphere with inner and outer radius, a and b, respectively. The hollow sphere is initially at uniform concentration, C_0, and the outer surface concentration is maintained at constant concentration, C_1. If the boundary condition at the inner surface, $r = a$, is of Type I (i.e., the inner surface is not permeable to any species), the initial and boundary conditions would be

$$C|_{t=0} = C_0, \tag{1a}$$

$$\left.\frac{\partial C}{\partial r}\right|_{r=a} = 0, \tag{1b}$$

$$C|_{r=b} = C_1. \tag{1c}$$

On putting $x = \frac{r-a}{b-a}$, $\tau = \frac{Dt}{(b-a)^2}$, and $u = \frac{(C-C_0)r}{(C_1-C_0)b}$, Eq. (1) becomes

$$\frac{\partial u}{\partial \tau} = \frac{\partial^2 u}{\partial x^2} \tag{2}$$

with

$$u|_{\tau=0} = 0, \tag{2a}$$

$$\left.\left(\frac{\partial u}{\partial x} - hu\right)\right|_{x=0} = 0, \tag{2b}$$

$$u|_{x=1} = 1, \tag{2c}$$

where $h = \frac{b}{a} - 1$.

Equation (2) can be solved using the method of separation of variables, and the solution to Eq. (2) in the

form of a trigonometrical series is

$$u(x,\tau)=\frac{hx+1}{h+1}-\sum_{n=1}^{\infty}\frac{\alpha_n}{\beta_n}\times\left[\sin(\lambda_n x)+\frac{\lambda_n}{h}\cos(\lambda_n x)\right]e^{-\lambda_n^2\tau}, \quad (3)$$

where

$$\alpha_n=\frac{1}{h+1}\left[\left(1+\frac{1}{h}+\frac{h}{\lambda_n^2}\right)\sin\lambda_n-\frac{h}{\lambda_n}\cos\lambda_n\right] \quad (4)$$

and

$$\beta_n=\frac{1}{2h^2}\left[\lambda_n^2+h^2+\frac{\lambda_n^2-h^2}{2\lambda_n}\sin(2\lambda_n)+2h\sin^2\lambda_n\right], \quad (5)$$

in which $\lambda_n (n=1,2,3,\ldots,\infty)$ are the positive roots of the following equation

$$\tan\lambda_n=-\frac{\lambda_n}{h}. \quad (6)$$

(Details are given in the Appendix.)

The fractional uptake, $\frac{\bar{q}_t}{q_\infty}$, is the ratio of the total amount of diffusing species that has entered the hollow sphere at time t, to the corresponding quantity after infinite time, i.e.,

$$\frac{\bar{q}_t}{q_\infty}=\frac{\int_a^b (C-C_0)\,4\pi r^2\,dr}{\int_a^b (C_1-C_0)\,4\pi r^2\,dr}. \quad (7)$$

The final expression for the fractional uptake by a hollow sphere with Type I boundary condition is

$$\frac{\bar{q}_t}{q_\infty}=1-\frac{3(h+1)^2}{h^2+3h+3}\sum_{n=1}^{\infty}\frac{\alpha_n^2}{\beta_n}e^{-\frac{\lambda_n^2 Dt}{\left(\frac{hb}{h+1}\right)^2}}. \quad (8)$$

In the case of Type II boundary condition, the concentration at the inner surface, $r=a$, is also kept at C_1 instead of a non-permeable surface. Although this type of boundary condition is less realistic, the expressions for $u(x,\tau)$ and fractional uptake can be obtained following a procedure similar to that described in the Appendix:

$$u(x,\tau)=\frac{hx+1}{h+1}-\frac{2}{\pi}\sum_{n=1}^{\infty}\frac{1}{n}\left[\frac{1}{h+1}-(-1)^n\right]\times\sin(n\pi x)e^{-n^2\pi^2\tau}, \quad (9)$$

$$\frac{\bar{q}_t}{q_\infty}=1-\frac{6}{\pi^2}\sum_{n=1}^{\infty}\frac{1}{n^2}\frac{[h+1-(-1)^n]^2}{h^2+3h+3}e^{-\frac{n^2\pi^2 Dt}{\left(\frac{hb}{h+1}\right)^2}}. \quad (10)$$

Equations (9) and (10) are essentially the same as those given by Crank (1975).

The hollow sphere becomes a solid sphere if $a=0$ (or $h\to\infty$). The corresponding expressions for the concentration of diffusing species, $C(r,t)$, and fractional uptake can be obtained by evaluating the limits of Eqs. (9) and (10) or Eqs. (3) and (8) as $h\to\infty$:

$$\frac{C(r,t)-C_0}{C_1-C_0}=1-\frac{2b}{\pi r}\sum_{n=1}^{\infty}\frac{(-1)^{n-1}}{n}\times\sin\left(\frac{n\pi r}{b}\right)e^{-\frac{Dn^2\pi^2 t}{b^2}}, \quad (11)$$

$$\frac{\bar{q}_t}{q_\infty}=1-\frac{6}{\pi^2}\sum_{n=1}^{\infty}\frac{1}{n^2}e^{-\frac{Dn^2\pi^2 t}{b^2}}. \quad (12)$$

Equations (11) and (12) are the well-known expressions for diffusion in a sphere (Crank, 1975).

Evaluation of the Equivalent Radius of Hollow Spheres

It is often convenient to evaluate the equivalent spherical particle radius, by means of which the effective diffusion rate or mass transfer coefficient in a hollow sphere can be analyzed easily and compared with those in a sphere. Usually, the equivalent spherical particle radius is taken as the radius of the sphere that has the same external surface to volume ratio (Kärger and Ruthven, 1992). However, our analysis showed that for a hollow sphere this treatment would underestimate the dimensionless time constant, r^2/D, by about 15%. A more rigorous method is given here to evaluate the equivalent spherical particle radius based on the theoretical expressions of the uptake curves.

The equivalent spherical particle radius, R, of a hollow sphere with an uptake curve given by Eq. (8), should be the radius in the uptake curve equation for a solid sphere (Eq. (12)), by means of which Eq. (12) could best match Eq. (8). The uptake curves for a hollow sphere and a solid sphere will be denoted by $(\frac{\bar{q}_t}{q_\infty})_{hs}$ and $(\frac{\bar{q}_t}{q_\infty})_s$, respectively, i.e.,

$$\left(\frac{\bar{q}_t}{q_\infty}\right)_{hs}=1-\frac{3(h+1)^2}{h^2+3h+3}\sum_{n=1}^{\infty}\frac{\alpha_n^2}{\beta_n}e^{-\frac{\lambda_n^2 Dt}{\left(\frac{hb}{h+1}\right)^2}}, \quad (13)$$

$$\left(\frac{\bar{q}_t}{q_\infty}\right)_s = 1 - \frac{6}{\pi^2}\sum_{n=1}^{\infty}\frac{1}{n^2}e^{-\frac{n^2\pi^2 Dt}{(pb)^2}}, \tag{14}$$

where the dimensionless equivalent radius, p, is defined as the ratio of the equivalent radius to the outer radius,

$$p = \frac{R}{b}. \tag{15}$$

To determine the equivalent spherical particle radius, we should adjust the parameter p in such a way that the difference between the two uptake curves is minimized. One way to evaluate the error as a result of expressing the uptake curve for a hollow sphere by the uptake equation for a sphere, $E(p)$, is

$$E(p) = \int_0^\infty \left[\left(\frac{\bar{q}_t}{q_\infty}\right)_s - \left(\frac{\bar{q}_t}{q_\infty}\right)_{hs}\right]^2 dt. \tag{16}$$

The parameter p can be determined by solving the following equation:

$$\frac{\partial}{\partial p}E(p) \equiv F(p) = 0. \tag{17}$$

$F(p)$ can be derived by substituting Eqs. (13)–(15) into Eq. (16):

$$F(p) = \frac{144pb^2}{D}\sum_{n=1}^{\infty}\sum_{m=1}^{\infty}\left\{\frac{1}{[n(n^2+m^2)\pi^3]^2} - \frac{\left[\left(1+\frac{1}{h}+\frac{h}{\lambda_n^2}\right)\sin\lambda_n - \frac{h}{\lambda_n}\cos\lambda_n\right]^2}{\left(1+\frac{3}{h}+\frac{3}{h^2}\right)\left[\lambda_n^2+h^2+\frac{\lambda_n^2-h^2}{2\lambda_n}\sin 2\lambda_n + 2h\sin^2\lambda_n\right]\left[\left(1+\frac{1}{h}\right)^2\lambda_n^2p^2+m^2\pi^2\right]^2}\right\}. \tag{18}$$

For a hollow sphere with a given outer radius, b, and $h(h=\frac{b}{a}-1)$, λ_n can be obtained using Eq. (6). With b, h, and λ_n, the equivalent radius, R, can be determined by solving Eq. (17). The expression, $F(p)$, for Type II boundary condition is as follows:

$$F(p) = \frac{144pb^2}{\pi^6 D}\sum_{n=1}^{\infty}\sum_{m=1}^{\infty}\frac{1}{n^2} \times \left\{\frac{1}{(n^2+m^2)^2} - \frac{[(h+1)-(-1)^n]^2}{(h^2+3h+3)\left[\left(1+\frac{1}{h}\right)^2n^2p^2+m^2\right]^2}\right\}. \tag{19}$$

Plane Sheet and Cylinder

For a solid plane sheet in the region, $-b < r < b$, initially at uniform concentration, C_0, and with the surfaces kept at constant concentration, C_1, the solution to the diffusion equation,

$$\frac{\partial C}{\partial t} = D\frac{\partial^2 C}{\partial r^2}, \tag{20}$$

in the form of a trigonometrical series, reads as

$$\frac{C(r,t)-C_0}{C_1-C_0} = 1 - \frac{4}{\pi}\sum_{n=0}^{\infty}\frac{(-1)^n}{2n+1} \times \cos\frac{(2n+1)\pi r}{2b}e^{-\frac{D(2n+1)^2\pi^2 t}{4b^2}}, \tag{21}$$

and the fractional uptake is

$$\frac{\bar{q}_t}{q_\infty} = 1 - \frac{8}{\pi^2}\sum_{n=0}^{\infty}\frac{1}{(2n+1)^2}e^{-\frac{D(2n+1)^2\pi^2 t}{4b^2}}. \tag{22}$$

The concentration expression of a hollow plane sheet in the region, $-b < r < -a$, and, $a < r < b$, with constant concentration both at the inner and outer surfaces, is the same as shown in Eq. (21), except that the half-thickness, b, should be replaced by $(b-a)/2$. In other words, the equivalent half-thickness, R, for the plane sheet with Type II boundary condition is

$$R = \frac{b-a}{2}. \tag{23}$$

Since the concentration gradient is zero in the central plane of a solid plane sheet, Eq. (21) is still valid if the inner surface of the hollow plane sheet is impermeable. In this case, the half-thickness should be replaced by the difference, $b-a$, and the equivalent half-thickness for the plane sheet with Type I boundary

condition is

$$R = b - a. \tag{24}$$

This consideration leads straightforwardly to the result that for hollow plates as compared with solid ones, the only difference between the diffusional processes compared to each other, comprises a time shift. This time shift can be expressed in terms of effective diffusion coefficients: $D/(b-a)^2$ versus $4D/(b-a)^2$.

The diffusion in the radial direction inside a cylinder can be described by

$$\frac{\partial C}{\partial t} = D\left(\frac{\partial^2 C}{\partial r^2} + \frac{1}{r}\frac{\partial C}{\partial r}\right). \tag{25}$$

If the surface concentration of the cylinder, which is initially at the value, C_0, is maintained at C_1, the solution to Eq. (25) is

$$\frac{C(r,t) - C_0}{C_1 - C_0} = 1 - \frac{2}{b}\sum_{n=1}^{\infty} \frac{J_0(r\alpha_n)}{\alpha_n J_1(b\alpha_n)} e^{-D\alpha_n^2 t}, \tag{26}$$

where b is the radius of the cylinder, and $J_0(x)$ and $J_1(x)$ represent the Bessel functions of the first kind of orders 0 and 1, respectively. The parameters, α_n, are the positive roots of the following equation:

$$J_0(b\alpha_n) = 0. \tag{27}$$

The corresponding uptake curve is expressed by

$$\frac{\bar{q}_t}{q_\infty} = 1 - \frac{4}{b^2}\sum_{n=1}^{\infty} \frac{1}{\alpha_n^2} e^{-D\alpha_n^2 t}. \tag{28}$$

Carslaw and Jaeger (1959) gave the general solution to the problem of a hollow cylinder under the condition of a uniform initial concentration profile, C_0. If both inner surface, $r = a$, and outer surface, $r = b$, are maintained at constant concentration (Type II), the solution to Eq. (25) reads as follows:

$$\frac{C(r,t) - C_0}{C_1 - C_0} = 1 - \pi \times \sum_{n=1}^{\infty} \frac{J_0(a\alpha_n)[Y_0(b\alpha_n)J_0(r\alpha_n) - J_0(b\alpha_n)Y_0(r\alpha_n)]}{J_0(a\alpha_n) + J_0(b\alpha_n)} e^{-D\alpha_n^2 t}, \tag{29}$$

where $Y_0(x)$ is the Bessel function of the second kind of order 0, and the parameters, α_n, are the positive roots of the following equation:

$$J_0(a\alpha_n)Y_0(b\alpha_n) - Y_0(a\alpha_n)J_0(b\alpha_n) = 0. \tag{30}$$

The expression for the amount of diffusing species entering (or leaving) the region, $a \le r \le b$, is (Crank, 1975):

$$\frac{\bar{q}_t}{q_\infty} = 1 - \frac{4}{b^2 - a^2}\sum_{n=1}^{\infty} \frac{J_0(a\alpha_n) - J_0(b\alpha_n)}{\alpha_n^2[J_0(a\alpha_n) + J_0(b\alpha_n)]} e^{-D\alpha_n^2 t}. \tag{31}$$

If the inner surface, $r = a$, is impermeable and the outer surface, $r = b$, is maintained at constant concentration (Type II), the solution to Eq. (25) reads as

$$\frac{C(r,t) - C_0}{C_1 - C_0} = 1 - \pi \times \sum_{n=1}^{\infty} \frac{J_1^2(a\alpha_n)[Y_0(b\alpha_n)J_0(r\alpha_n) - J_0(b\alpha_n)Y_0(r\alpha_n)]}{J_1^2(a\alpha_n) + J_0^2(b\alpha_n)} e^{-D\alpha_n^2 t}, \tag{32}$$

where the parameters, α_n, are the positive roots of the equation

$$J_1(a\alpha_n)Y_0(b\alpha_n) - Y_1(a\alpha_n)J_0(b\alpha_n) = 0, \tag{33}$$

and $Y_1(x)$ is the Bessel function of the second kind of order 1. The expression for the fractional uptake curve is given by

$$\frac{\bar{q}_t}{q_\infty} = 1 - \frac{4}{b^2 - a^2}\sum_{n=1}^{\infty} \frac{e^{-D\alpha_n^2 t}}{\alpha_n^2\left[1 - \frac{J_0^2(b\alpha_n)}{J_1^2(a\alpha_n)}\right]}. \tag{34}$$

Using the same method as shown earlier for a hollow sphere, the equivalent radius for a hollow cylinder with Type I boundary conditions can be evaluated using Eq. (17) with

$$F(p) = \frac{64b^2 p}{D}\sum_{n=1}^{\infty}\sum_{m=1}^{\infty}\left\{\frac{1}{\alpha_n^2\left(\alpha_n^2 + \alpha_m^2\right)^2} - \frac{J_1^2(a\beta_n)}{\beta_n^2(b^2 - a^2)\left[J_1^2(a\beta_n) - J_0^2(b\beta_n)\right]\left(b^2 p^2 \beta_n^2 + \alpha_m^2\right)^2}\right\}, \tag{35}$$

where p is the ratio of equivalent radius to the outer radius as defined by Eq. (15), and

$$J_0(\alpha_n) = 0, \tag{36}$$

$$J_1(a\beta_n)Y_0(b\beta_n) - Y_1(a\beta_n)J_0(b\beta_n) = 0. \tag{37}$$

For Type II boundary conditions, the expression for $F(p)$ in Eq. (17) is

$$F(p) = \frac{64b^2p}{D}\sum_{n=1}^{\infty}\sum_{m=1}^{\infty}\left\{\frac{1}{\alpha_n^2\left(\alpha_n^2+\alpha_m^2\right)^2} - \frac{J_0(a\beta_n) - J_0(b\beta_n)}{\beta_n^2(a^2-b^2)[J_0(a\beta_n)+J_0(b\beta_n)]\left(b^2p^2\beta_n^2+\alpha_m^2\right)^2}\right\}, \tag{38}$$

where

$$J_0(\alpha_n) = 0, \tag{39}$$

and

$$J_0(a\beta_n)Y_0(b\beta_n) - Y_0(a\beta_n)J_0(b\beta_n) = 0. \tag{40}$$

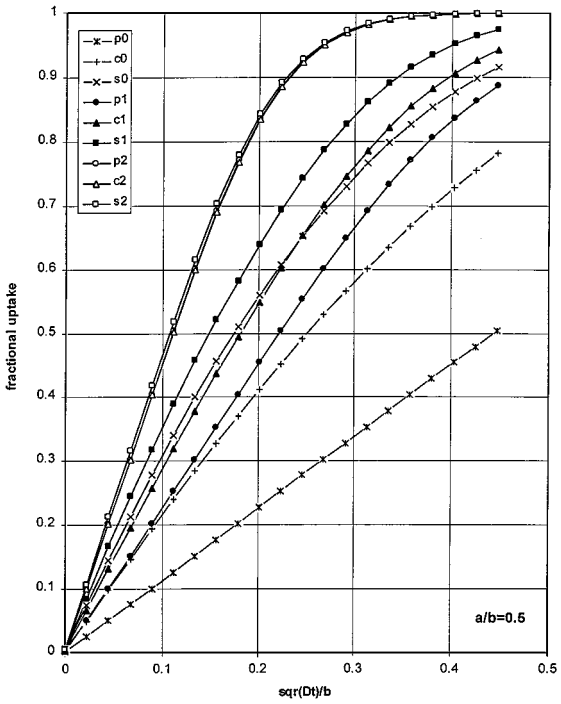

Figure 1. Uptake curves for diffusion in plane sheet, cylinder, and sphere of hollow (with $a/b = 0.5$) and solid geometries.

Comparison of Uptake Curves for Diffusion in Hollow Plane Sheet, Cylinder, and Sphere

To compare the uptake curves for the diffusion in hollow plane sheet, cylinder, and sphere, the fractional uptakes by the three hollow geometries are plotted against $(Dt/b^2)^{1/2}$ in Fig. 1. The letters, p, c, and s, in the legend stand for plane sheet, cylinder, and sphere, while the numbers, 0, 1, and 2, refer to the solid geometry, hollow geometry with Type I inner boundary condition, and hollow geometry with Type II inner boundary conditions, respectively. For all the cases shown in Fig. 1, the inner length, a, which is the distance from the center to the inner surface of the hollow geometry, was set equal to 50% of the outer length, b.

It is obvious that the diffusion in the solid geometry is slower than that in the hollow geometry because of the longer diffusion path in the solid geometry. Since a hollow sphere has the largest outer specific surface area (outer surface area per unit volume of material), the sphere shows the fastest and the plane sheet the slowest diffusion uptake, for both solid material and hollow material with non-permeable inner surface (Type I). If the inner surface is permeable (Type II), the uptake curves for a plane sheet and cylinder are nearly identical. This is consistent with the fact that the hollow plane sheet and cylinder have the same values of total specific surface area, $2/(b-a)$, if both inner and outer surfaces are included. Depending on the inner-to-outer radius ratio, a/b, the total specific surface area of a hollow sphere, $3(b^2+a^2)/(b^3-a^3)$, is by 0–50% higher than that for a hollow cylinder. When the ratio is 0.5 as in Fig. 1, the hollow sphere has by $\frac{1}{14}$ more total surface area than the hollow cylinder, and the sphere exhibits slightly faster uptake.

Equivalent Sizes of Hollow Plane Sheet, Cylinder, and Sphere

For simplicity, we will designate a common term-equivalent size-to equivalent radius (for hollow sphere and hollow cylinder) and equivalent half-thickness (for hollow plane sheet). The ratio of equivalent size, R, to the outer length, b, will be referred to as dimensionless equivalent size, p, as defined by Eq. (15). As mentioned earlier, the equivalent size, R, can be determined

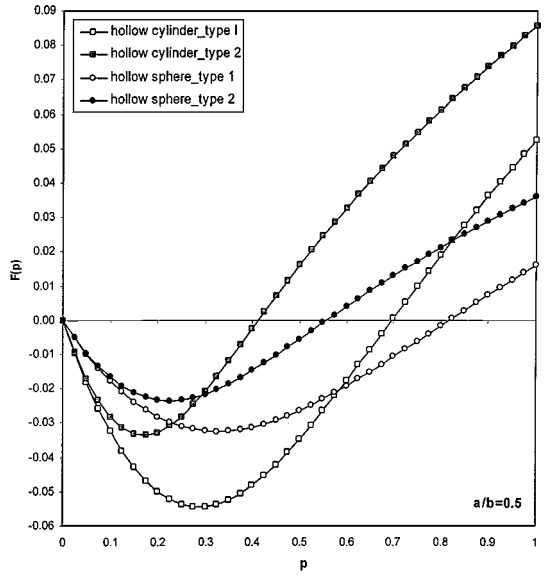

Figure 2. Function $F(p)$.

based on the uptake rate expressions for solid and hollow materials by solving Eq. (17). The function, $F(p)$, in Eq. (17) is the derivative of the error, $E(p)$, incurred when the uptake by a hollow material is expressed in terms of the uptake by its corresponding solid material.

The function $F(p)$ is represented in Fig. 2 for the cases of hollow cylinder and sphere for $a/b = 0.5$. As can be seen from Fig. 2, Eq. (17) has only one root between 0 and 1, except the trivial solution at $p = 0$. Since $F(p)$ changes from negative to positive values as p passes the single root, the function $E(p)$ has its minimum at $F(p) = 0$.

The concept of equivalent size parameter, R, is a useful tool for the evaluation of effectiveness and advantages of hollow materials in terms of diffusion or mass transfer rate. The equivalent size parameter of a hollow geometry discussed here is relative to its solid geometry of the same geometrical shape, and it is obtained based on the fractional uptake. One of the approximate ways to estimate the equivalent size is the equivalent spherical radius, R', based on the ratio of volume, V, to the external surface area, A, as discussed by Do (1998):

$$R' = \frac{3V}{A}. \tag{41}$$

Similar to the dimensionless equivalent size, the dimensionless equivalent spherical radius, p', can be defined as the ratio of the equivalent spherical radius, R', of a hollow geometry to that of its corresponding solid geometry. Table 1 compiles the equations for the equivalent spherical radii (based on Eq. (41)), the dimensionless equivalent spherical radii, and the dimensionless equivalent sizes of the three geometrical shapes considered in this paper.

It should be noted that the dimensionless equivalent size, p, is directly related to the diffusion rate, since its evaluation is based on the analysis of the fundamental diffusion equation. However, the calculation of dimensionless equivalent spherical radius, p', shown in Table 1 is based on specific surface area, and it should, therefore, be regarded as an approximation of the dimensionless equivalent size. As can be seen from

Table 1. The dimensionless equivalent size and dimensionless equivalent spherical radius for hollow geometries.

Shape	Inner surface	R'	p'	p
Plane sheet (P)	Non-permeable (Type I)	$3(b-a)$	$1-\frac{a}{b}$	$1-\frac{a}{b}$, (Eq. (24))
	Permeable (Type II)	$\frac{3}{2}(b-a)$	$\frac{1}{2}(1-\frac{a}{b})$	$\frac{1}{2}(1-\frac{a}{b})$, (Eq. (23))
Cylinder (C)	Non-permeable (Type I)	$\frac{3}{2}(b-\frac{a^2}{b})$	$1-\frac{a^2}{b^2}$	(Eq. (35))
	Permeable (Type II)	$\frac{3}{2}(b-a)$	$1-\frac{a}{b}$	(Eq. (38))
Sphere (S)	Non-permeable (Type I)	$b-\frac{a^3}{b^2}$	$1-\frac{a^3}{b^3}$	(Eq. (18))
	Permeable (Type II)	$(b-\frac{a^3}{b^2})/(1+\frac{a^2}{b^2})$	$(1-\frac{a^3}{b^3})/(1+\frac{a^2}{b^2})$	(Eq. (19))

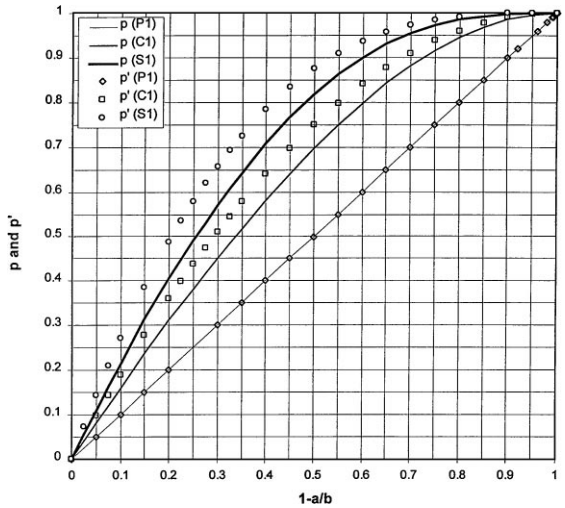

Figure 3. Dimensionless equivalent size parameters of hollow materials with non-permeable inner surface.

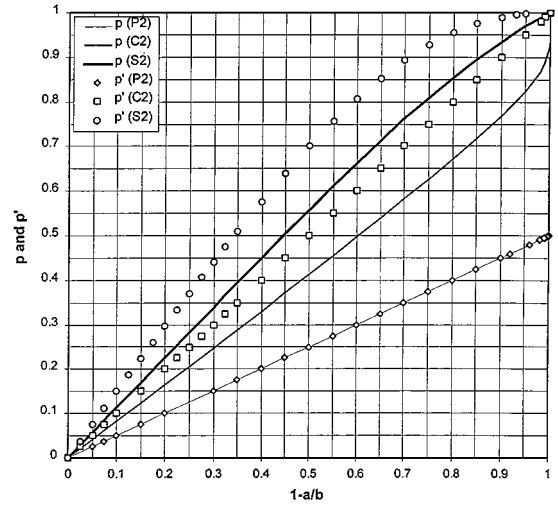

Figure 4. Dimensionless equivalent size parameters of hollow materials with permeable inner surface.

Figs. 3 and 4, the difference between the size parameters, p and p', can be as high as 15%.

The size parameters, p and p', are shown in Fig. 3, as functions of the dimensionless wall thickness, $1-a/b$, for plane sheet, cylinder, and sphere with non-permeable inner surface (Type I). For hollow plane sheet, the parameters, p and p', are the same and are equal to the dimensionless wall thickness, $1-a/b$. That is to say that diffusion in a hollow plane sheet with non-permeable inner surface is equivalent to that in a solid sheet that has a half-thickness equal to the wall thickness of the hollow sheet. The equivalent size for a hollow cylinder or a hollow sphere is greater than its wall thickness. For the same dimensionless wall thickness, $1-a/b$, the hollow sphere has a larger equivalent size than the hollow cylinder. This is due to the more rapidly reduced cross-section area in a hollow sphere than that in a hollow cylinder, as the diffusing species moves towards the inner surface. A reduced cross-section area perpendicular to the direction of diffusion makes the diffusion process more difficult. Therefore, for the same wall thickness, the equivalent radius of a hollow sphere is greater than that of a cylinder.

Under the boundary condition of Type II, for which the inner surface is permeable and both inner and outer surfaces are kept at constant concentration, diffusion proceeds from both surfaces of the hollow material. As shown in Fig. 4, the equivalent sizes of all the three geometrical shapes are reduced because of the increased diffusion rate. Since the cross-section area of a plane sheet is constant in the diffusion direction, the equivalent half-thickness for a hollow plane sheet is reduced by 50% compared to the hollow plane sheet with non-permeable inner surface. The equivalent radius for a hollow cylinder is less than its wall thickness. For a hollow sphere, however, the equivalent radius is still larger than its wall thickness.

Mass Transfer Rates in Hollow and Solid Materials

In diffusion-controlled systems, the mass transfer behavior is often simplified to a 'linear-driving force approximation' (Glueckauf and Coates, 1947; Glueckauf, 1955), in which the mass transfer coefficient (or the effective diffusion rate) is assumed to be inversely proportional to the square of radius of an equivalent sphere. Using the concept of equivalent size as discussed earlier, one could quantify the effective mass transfer rate in hollow materials relative to those in solid materials.

The gain in mass transfer rate (or in the particle mass transfer coefficient) due to hollowness of a material relative to its corresponding solid material is exemplified in Figs. 5 and 6, as a function of hollow volume percentage, for the two types of inner boundary conditions. As shown in Figs. 2–4, for the same wall thickness, the sphere shows the largest equivalent length among the three geometrical shapes considered. However, for the same hollow volume percentage, the hollow sphere with non-permeable inner surface gains more in mass transfer rate than the plane sheet and the hollow cylinder. For the permeable inner surface, there exists

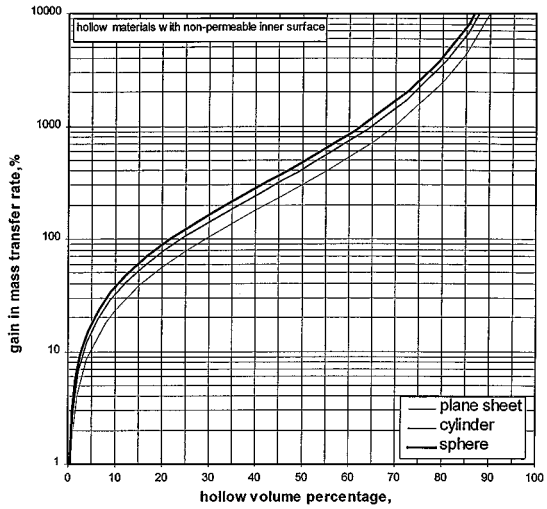

Figure 5. Mass transfer rate gain by hollow materials with non-permeable inner surface.

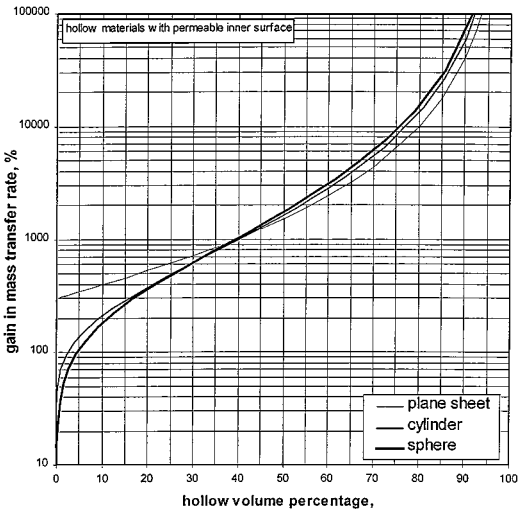

Figure 6. Mass transfer rate gain by hollow materials with permeable inner surface.

a cross point at a hollow volume percentage of about 27%, above which the hollow sphere gives the higher gain in mass transfer rate than the hollow cylinder.

Real sorbent media such as crystals of microporous materials may comprise solid particles of various geometric shapes. In addition to the hollow particles considered here, there might be hollow particles with perforations that serve as 'connecting passages'. In the real cases, the hollow particles as well as the ones with connecting passages result from accidental or deliberate modification that take place during synthesis and/or further treatment of appropriately chosen classes of materials (Franklin and Lowe, 1987). In particular, they may represent defect structures caused by alkaline or acid leaching of their inner lattice bulks, or intentionally synthesized gel particle zeolites such as silicalite-1 (Franklin and Lowe, 1987). An account for the existence of 'connecting passages' in hollow geometries may be another development of ideas outlined in this paper. Its influence should lead to additional enhancement of mass transport.

Conclusions

The equivalent sizes (or diffusion lengths) of diffusing species for hollow geometries of a material compared to their corresponding geometries of a solid material were evaluated directly from the analytical expressions of the fractional uptake rate curves. For the same hollow volume fraction, the sphere shows the highest and the plane sheet the lowest gain in effective diffusion rate. The result may have practical implications for sorption processes in fluid-(porous) solid systems.

Appendix: Solution of the Equation for the Diffusion in Hollow Sphere

The general solution to Eq. (2) in the form of a trigonometrical series is

$$u(x,\tau) = f(x) + \sum_{n=1}^{\infty} \times [A_n \sin(\lambda_n x) + B_n \cos(\lambda_n x)]\, e^{-\lambda_n^2 \tau}, \tag{A1}$$

with $f(x)$ as a linear function of x. Since the concentration of diffusing species anywhere inside the hollow sphere after infinite time (i.e., $\tau \to \infty$) approaches the value, C_1, the limits of u as $\tau \to \infty$ at the inner and outer surfaces, are $u(0,\infty) = \frac{a}{b} = \frac{1}{h+1}$ and $u(1,\infty) = 1$, respectively. Considering the fact that the second term in Eq. (A1) becomes zero as $\tau \to \infty$, the linear term, $f(x)$, in the general solution expression (Eq. (A1)) should be

$$f(x) = \frac{hx+1}{h+1}, \tag{A2}$$

and the general solution to Eq. (2) becomes

$$u(x,\tau) = \frac{hx+1}{h+1} + \sum_{n=1}^{\infty} \times [A_n \sin(\lambda_n x) + B_n \cos(\lambda_n x)] e^{-\lambda_n^2 \tau}, \tag{A3}$$

where A_n, B_n, and λ_n are determined by the initial and boundary conditions.

From the boundary condition at $x = 0$, we have

$$\left(\frac{\partial u}{\partial x} - hu\right)\Big|_{x=0} = \sum_{n=1}^{\infty}(\lambda_n A_n - h B_n)e^{-\lambda_n^2 \tau} = 0, \tag{A4}$$

which can be satisfied only if

$$\lambda_n A_n - h B_n = 0. \tag{A5}$$

B_n can be expressed by

$$B_n = \frac{\lambda_n A_n}{h}. \tag{A6}$$

From the boundary condition at $x = 1$, we have

$$\sum_{n=1}^{\infty}(A_n \sin\lambda_n + B_n \cos\lambda_n)e^{-\lambda_n^2 \tau} = 0 \tag{A7}$$

or

$$A_n \sin\lambda_n + B_n \cos\lambda_n = 0. \tag{A8}$$

Substituting Eq. (A6) into Eq. (A8) gives

$$\tan\lambda_n = -\frac{\lambda_n}{h}. \tag{A9}$$

Applying the initial condition (Eq. (2a)) to Eq. (A3) results in

$$\frac{hx+1}{h+1} + \sum_{n=1}^{\infty} A_n\left[\sin(\lambda_n x) + \frac{\lambda_n}{h}\cos(\lambda_n x)\right] = 0 \tag{A10}$$

or

$$-f(x) = \sum_{n=1}^{\infty} A_n F_n(x), \tag{A11}$$

where

$$F_n(x) = \sin(\lambda_n x) + \frac{\lambda_n}{h}\cos(\lambda_n x). \tag{A12}$$

For any two eigenvalues λ_m and $\lambda_n (\lambda_m \neq \lambda_n)$,

$$F_m'' + \lambda_m^2 F_m = 0, \tag{A13a}$$

$$F_n'' + \lambda_n^2 F_n = 0. \tag{A13b}$$

This boundary value problem is called a *Sturm-Liouville* problem (Kreyszig, 1989). Multiplying Eq. (A13a) by F_n and Eq. (A13b) by F_m followed by subtracting the resulting Eq. (A13b) from Eq. (A13a) yields

$$(\lambda_m^2 - \lambda_n^2)F_m F_n = F_m F_n'' - F_n F_m''. \tag{A14}$$

Integrating Eq. (A14) gives

$$(\lambda_m^2 - \lambda_n^2)\int_0^1 F_m F_n\, dx = [F_m F_n' - F_n F_m']_{x=0}^{x=1}. \tag{A15}$$

It can be shown that the r.h.s. of Eq. (A15) is zero. Since $\lambda_m \neq \lambda_n$, the integral on the l.h.s. of Eq. (A15) must be zero. In other words, if $\lambda_m \neq \lambda_n$, we have the orthogonality condition:

$$\int_0^1 F_m(x) F_n(x)\, dx = 0. \tag{A16}$$

With the help of Eq. (A16), A_n can be obtained by multiplying Eq. (A11) by $F_m(x)$, integrating between 0 and 1, and solving for A_n:

$$A_n = -\frac{\alpha_n}{\beta_n}, \tag{A17}$$

where

$$\alpha_n \equiv \int_0^1 f(x)F_n(x)\, dx = \frac{1}{h+1}\left[\left(1 + \frac{1}{h} + \frac{h}{\lambda_n^2}\right)\sin\lambda_n - \frac{h}{\lambda_n}\cos\lambda_n\right] \tag{A18}$$

and

$$\beta_n \equiv \int_0^1 F_n^2(x)\, dx = \frac{1}{2h^2}\left[\lambda_n^2 + h^2 + \frac{\lambda_n^2 - h^2}{2\lambda_n}\sin(2\lambda_n) + 2h\sin^2\lambda_n\right]. \tag{A19}$$

It follows from Eqs. (A6) and (A17) that

$$B_n = -\frac{\lambda_n \alpha_n}{h\beta_n}. \tag{A20}$$

Therefore, the solution to Eq. (2) can be written as

$$u(x,\tau) = \frac{hx+1}{h+1} - \sum_{n=1}^{\infty} \frac{\alpha_n}{\beta_n} \times \left[\sin(\lambda_n x) + \frac{\lambda_n}{h} \cos(\lambda_n x) \right] e^{-\lambda_n^2 \tau}, \quad \text{(A21)}$$

in which $\lambda_n (n = 1, 2, 3, \ldots, \infty)$ are the positive roots of Eq. (A9), and α_n and β_n are calculated by Eqs. (A18) and (A19).

Nomenclature

A	Surface area;
A_n	Coefficient (Eq. (A1));
a	Inner radius (for hollow sphere and hollow cylinder) or inner half-thickness;
B_n	Coefficient (Eq. (A1));
b	Outer radius (for hollow sphere and hollow cylinder) or outer half-thickness;
C	Concentration of diffusing species;
C_0	Initial concentration of diffusing species;
C_1	Surface concentration of diffusing species;
D	Diffusion coefficient;
$E(p)$	Function defined by Eq. (17);
$F_n(x)$	Function defined by Eq. (A12);
F_n'	First derivative of function $F_n(x)$;
F_n''	Second derivative of function $F_n(x)$;
$F(p)$	First derivative of $E(p)$;
$f(x)$	Function defined by Eq. (A2);
h	Constant, $h = \frac{b}{a} - 1$;
$J_0(x)$	Bessel function of the first kind of order 0;
$J_1(x)$	Bessel function of the first kind of order 1;
m	Integer;
n	Integer;
p	Dimensionless equivalent size parameter, $p = \frac{R}{b}$;
p'	Dimensionless equivalent spherical radius, $p' = \frac{R'}{b}$;
$\bar{q}_t$	The total amount of diffusing species that has entered the region between inner surface and outer surface at time t;
q_∞	The total amount of diffusing species that has entered the region between inner surface and outer surface after infinite time;
R	Equivalent size parameter;
R'	Equivalent spherical radius;
r	Space coordinate along the direction of diffusion;
t	Time;
u	Dimensionless concentration;
V	Volume;
x	Dimensionless space coordinate, $x = \frac{r-a}{b-a}$;
$Y_0(x)$	Bessel function of the second kind of order 0;
$Y_1(x)$	Bessel function of the second kind of order 1;
α_n	Parameter defined by Eqs. (A18), (27), (30), (33), (36), and (39);
β_n	Parameter defined by Eqs. (A19), (37), and (40);
λ_n	Parameter defined by Eq. (6) (or Eq. (A9));
τ	Dimensionless time, $\tau = \frac{Dt}{(b-a)^2}$.

References

Barrer, R.M., "Diffusion in Spherical Shells and a New Method of Measuring the Thermal Diffusivity Constant," *Phil. Mag.*, **35**, 802 (1944).

Carslaw, H.S. and J.C. Jaeger, *Conduction of Heat in Solids*, 2nd ed., pp. 246, 333, Oxford University Press, 1959.

Crank, J., *The Mathematics of Diffusion*, 2nd ed., pp. 83, 91, 98, Oxford University Press, 1975.

Do, D.D., *Adsorption Analysis: Equilibria and Kinetics*, p. 555, Imperial College Press, London, 1998.

Franklin, K.R. and B.M. Lowe, "Preparation and Properties of Gel Particle Silicalite," *Zeolites*, **7**, 135–142 (1987).

Glueckauf, E., "Theory of Chromatography, Part 10.—Formulae for Diffusion into Spheres and Their Application to Chromatography," *Trans. Faraday Soc.*, **51**, 1540–1551 (1955).

Glueckauf, E. and J.E. Coates, "Theory of Chromatography. Part IV.—The Influence of Incomplete Equilibrium on the Front Boundary of Chromatograms and on the Effectiveness of Separation," *J. Chem. Soc.*, 1315–1321 (1947).

Goto, M. and T. Hirose, "Approximations of Diffusion Processes for a Particle with Inner Core," *J. Chem. Eng. Japan*, **27**(4), 544–547 (1994).

Hublitz, R. and U. Birkenstock, "Verfahren zur Herstellung Keramischer Formkörper," DE 3,826,220, Hoechst CeramTec AG and Bayer AG, February 8, 1990.

Hunold, K., Th. Kempf, and A. Lipp, "Polykristalline Sinterkörper auf Basis von Aluminumnitrid und Verfahren zu ihrer Herstellung," DE 3,743,663 A1, Elektroschmelzwerk Kempten, May 7, 1989.

Kärger, J. and D.M. Ruthven, *Diffusion in Zeolites and Other Microporous Solids*, p. 238, John Wiley & Sons, Inc., New York, 1992.

Kreyszig, E., *Advanced Engineering Mathematics*, 5th ed., pp. 188–192, Wiley Eastern Ltd., New Delhi, 1989.

Nippon Steel Corp., "Ceramic Composite and Process for Preparation Thereof," EP 0,308,873 A2, March 1987.

Papa, J., Y.T. Shah, A. Frost, and J. Sawyer, "Role of Support Structure on Kinetic Parameter Estimations in a Shell Catalyst," *Chem. Eng. Commun.*, **110**, 71–83 (1991).

Pereira, C.J. and L. Hegedus, "Extrudat und Katalysator mit einer hohen geometrischen Oberfläche," EP 0,141,997 A1, EP 0,141,998 A1, W.R. Grace & Co., May 22, 1985.

Shell Internationale, "Silica extrudates," EP 0,309,048 A1, March 1989.

Seki, Y., S. Ose, and H. Kodama, "Manufacture of Microporous Ceramic Articles," Jpn. Kokai Tokkyo Koho JP 01,172,283 (89,172,283), Agency of Industrial Sciences and Technology, July 7, 1989.

Sextl, E. and P. Kleinschmit, "Molded Bodies Containing Dealuminated Zeolite Y and the Process for Their Production," US Patent 5,316,993, Degussa AG, May 31, 1994.

Siebers, F., W. Kiefer, and M. Sura, "Verfahren zur Herstellung von offenporigen Sinterkörpern," DE 3,731,649 A1, Schott Glaswerke, March 30, 1989.

Sovova, H., "Rate of the Vegetable Oil Extraction with Supercritical CO_2—I. Modeling of Extraction Curves," *Chem. Eng. Sci.*, **49**, 409–414 (1994).

Takahashi, A., M. Shilahara, K. Morimoto, M. Samma, and O. Kubo, "Formkörper aus Kieselsäure," EP 0,236,498, Kabushiki Kaishi Osaka, February 7, 1990.

Tatlier, M. and A. Erdem-Senatalar, "Optimization of the Thickness of Zeolite 4A Coatings on Metal Surfaces for Heat Pump Applications," in *Proc. 12th International Zeolite Conference* 1999, MRS, Vol. 1, pp. 583–590.

Tosheva, L., V. Valtchev, and J. Sterte, "Bilayered Hollow Zeolite Tubes," in *Proc. 12th International Zeolite Conference* 1999, MRS, Vol. 1, pp. 629–635.

Unger, K.K.A., "Handbuch der HPLC, Teil 1: Leitfaden für Anfänger und Praktiker," Kapitel 3, GIT Verlag, Darmstadt, 1989.

van der Eerden, A.M.J., D.C. Koningsberger, and J.W. Geus, "Growth of Zeolites Firmly Attached to Metal Surfaces for Use in Catalysis," in *Proc. 12th International Zeolite Conference* 1999, MRS, Vol. 1, pp. 637–642.